Electronic Supplementary Information (ESI) for

Hierarchical porous Ni, Fe-codoped Co-hydroxide arrays derived from metal-organic-framework for Enhanced Oxygen Evolution

Qian Ren, Jin-Qi Wu, Cheng-Fei Li, Lin-Fei Gu, Ling-Jie Xie, Yu Wang, Gao-Ren Li*

MOE Key Laboratory of Bioinorganic and Synthetic Chemistry, School of Chemistry, Sun Yat-Sen University, Guangzhou 510275, China.

Materials and Methods

Cobalt(II) nitrate hexahydrate ($Co(NO_3)_2 \cdot 6H_2O$, 99.99%), Iron(II) chloride tetrahydrate ($FeCl_2 \cdot 4H_2O$, 99.95%), Zinc(II) nitrate hexahydrate ($Zn(NO_3)_2 \cdot 6H_2O$, 99%), 1,3,5-benzenetricarboxylic acid ($C_6H_3(CO_2H)_3$, 98%), Sodium hydroxide (NaOH, 96%), Potassium hydroxide (KOH, 95%), Deionized (DI) water from a Millipore system (18.2 MΩ cm) was used for solution. Ni foam with a thickness of 0.3 mm was used. All chemical reagents used in this work were analytical grade (AR) with no further processing.

Synthesis of BTC-Co/NF.

The Ni foam (NF) ($3 \times 3 \times 0.1$ cm^2) was rinsed with ethanol to remove surface impurities, and then immersed in the hydrochloric acid (3 M HCl) solution to remove oxided nickel on surface, the obtained NF was washed repeatedly with distilled water. 80 mg of 1,3,5-Benzenetricarboxylic acid (H_3BTC) and 45 mg of NaOH were dissolved in 15 mL of deionized water to obtain a colorless solution (A solution), 0.8 mmol of $Co(NO_3)_2 \cdot 6H_2O$ was dissolved in other 10 mL of deionized water to obtain a pink solution (B solution). And then, A solution was added in B solution under continuous stirring to obtain a homogeneous solution. The above mixture solution and a piece of preprocessed NF were transferred to a Teflon-lined stainless-steel autoclave and maintained at 180 ˚C for 6 h. The purple BTC-Co on Ni foam

(named as BTC-Co/NF) was gained and washed with ethanol and distilled water for several times, dried at 60 ˚C.

Synthesis of BTC-CoZn/NF.

The preparation method is the same as the BTC-Co/NF procedure, except for replace 0.8 mmol of $Co(NO_3)_2 \cdot 6H_2O$ with 0.6 mmol of $Co(NO_3)_2 \cdot 6H_2O$ and 0.2 mmol of $Zn(NO_3)_2 \cdot 6H_2O$.

Synthesis of BTC-CoZnFeNi/NF.

The preparation method is the same as the BTC-Co/NF procedure, except for replace 0.8 mmol of $Co(NO_3)_2 \cdot 6H_2O$ with 0.4 mmol of $Co(NO_3)_2 \cdot 6H_2O$, 0.2 mmol of $Zn(NO_3)_2 \cdot 6H_2O$ and 0.2 mmol of $FeCl_2 \cdot 4H_2O$. Due to the acidity of $FeCl_2$ solution, under hydrothermal conditions, nickel foam was corroded resulting in Ni dissolution and doping into the product.

Synthesis of Co-H NAs/NF.

An electrochemical method was used to remove the ligand. The cyclic voltammetry (CV) mode with a fixed potential window of 0.925~1.475 V (*vs*. RHE) was performed in 1.0 M KOH, the scan rate is 10 mV s^{-1}. The BTC-CoZn/NF as precursor, after continuous CV cycle (10, 30, 50, and 100 cycles), the BTC-CoZn evolved into cobalt hydroxide. After 100 cycles, the final product was collected and labelled as Co-H NAs/NF.

Synthesis of $Ni_{0.8}Fe_{0.2}$/Co-H NAs/NF.

The preparation method is the same as the Co-H/NF procedure, except for replace the precursor BTC-CoZn/NF with BTC-CoZnFeNi/NF, the final product was collected and labelled as $Ni_{0.8}Fe_{0.2}$/Co-H NAs/NF, the ICP-AES data shows the molar ratio of Ni Fe is 0.8:0.2.

Characterizations

X-ray di□raction (PXRD) patterns were recorded on a Rigaku D/Max 2550 X-ray di□ractometer with a

Cu Kα radiation (40 kV-40 mA). The surface morphologies of the products were characterized by Zeiss Sigma field emission scanning electron microscope (FE-SEM, Quanta 400FEG). The inner structures were characterized by transmission electron microscope (TEM, JEM-2010HR). The High-resolution TEM and Energy-dispersive X-ray spectroscopy (EDX) analysis were carried out on JEM-3010HR. Atomic force microscopy (AFM) images were performed by a SHIMDZU SPM-9500J3 device. The valence state analysis of the products was obtained by X-Ray photoelectron spectroscopy (XPS) using an ESCALAB 250 X-Ray photoelectron spectrometer, and all the XPS spectra peaks were corrected by C 1s line at 284.8 eV as standard. Molecular groups analysis of samples was determined by Fourier transform infrared (FTIR) spectra (Renishaw inVia). The inductively coupled plasma-atomic emission spectrometry (ICP-AES) was carried out on TJA IRIS (HR) spectrometer.

Electrochemical Measurements

All electrocatalysts measurements were acquired in a typical three-electrode configuration in the O_2-saturated solution at room temperature on a CHI 660D Electrochemical Workstation. In all electrochemical measurements, the as-prepared catalysts on NF were used as the working electrode (the area in the submerged electrolyte is 0.2 cm × 0.5 cm × 2), carbon rod as the counter electrode, and a Hg/HgO (1.0 M KOH) electrode as reference electrode. All potentials measured were converted to the reversible hydrogen electrode (RHE) adopting the following equation: E_{RHE} (V) = $E_{Hg/HgO}$ (V) + 0.098 V + 0.059 pH. The overpotential (η) was calculated from the formula: $\eta = E_{RHE} - 1.23$ V. The linear sweep voltammetry (LSV) was performed at a scan rate of 1 mV s^{-1} in 1.0 M KOH (pH 14) solution (the deionized water was used as solvent). All polarization curves were corrected with 95% iR-compensation. Electrochemical impedance spectroscopy (EIS) measurements were carried out at 1.524V (*vs*.RHE) in the frequency range of 100kHz~0.01Hz with 5 mV sinusoidal perturbations. Chronopotentiostatic

curves were recorded at a constant current density of 10 mA cm^{-2}. The double-layer capacitance (C_{dl}) via cyclic voltammograms (CV) at different scan rates of 10-50 mV s^{-1} were measured to estimate electrochemically active surface area (ECSA).

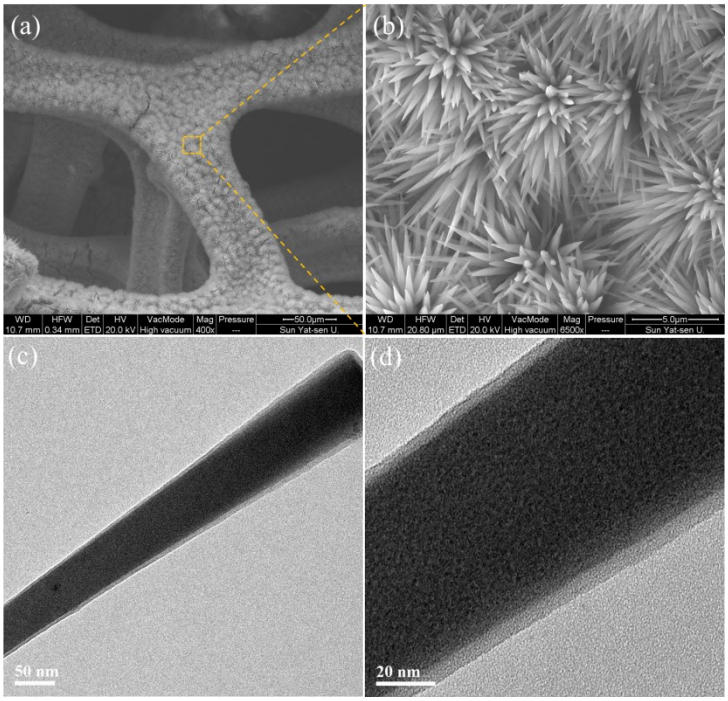

Fig. S1 (a,b) SEM images and (c,d) TEM images of BTC-Co/NF.

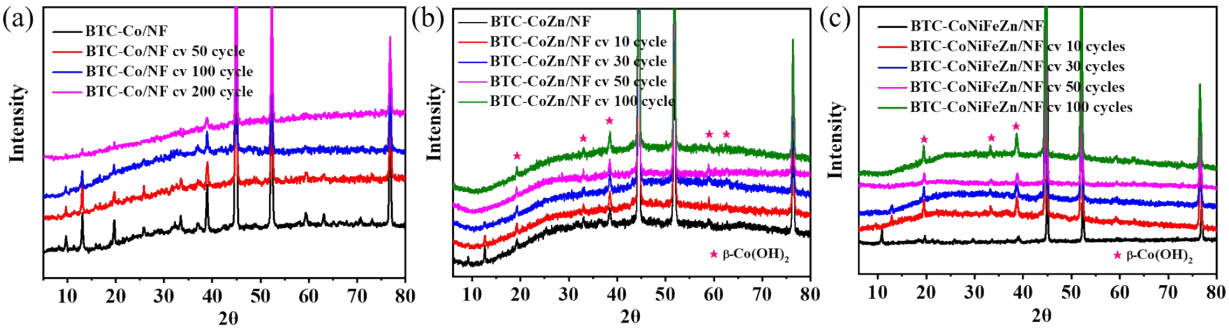

Fig. S2 XRD patterns of (a) BTC-Co/NF, (b) BTC-CoZn/NF, and (c) BTC-CoNiFeZn/NF before and after different CV treatments with a fixed potential window of 0.925~1.475 V (*vs*. RHE) in 1.0 M KOH.

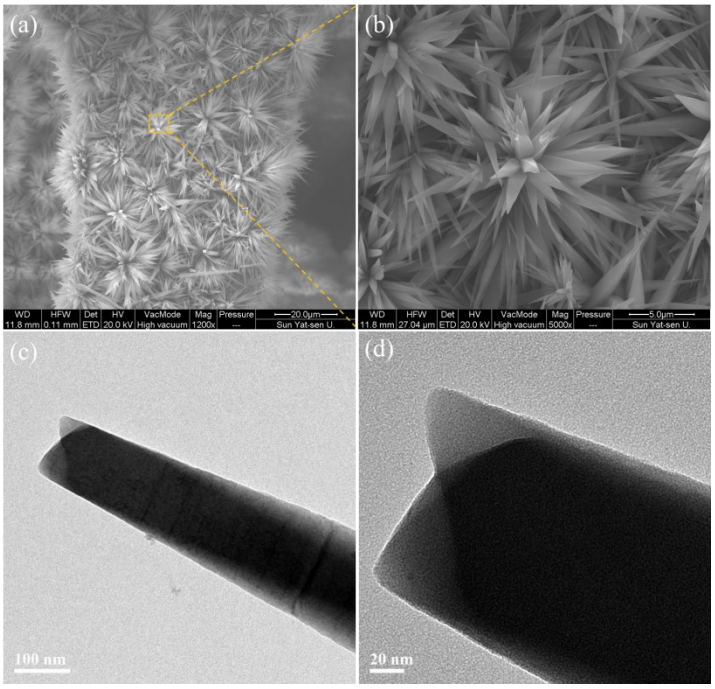

Fig. S3 (a,b) SEM images and (c,d) TEM images of BTC-CoZn/NF.

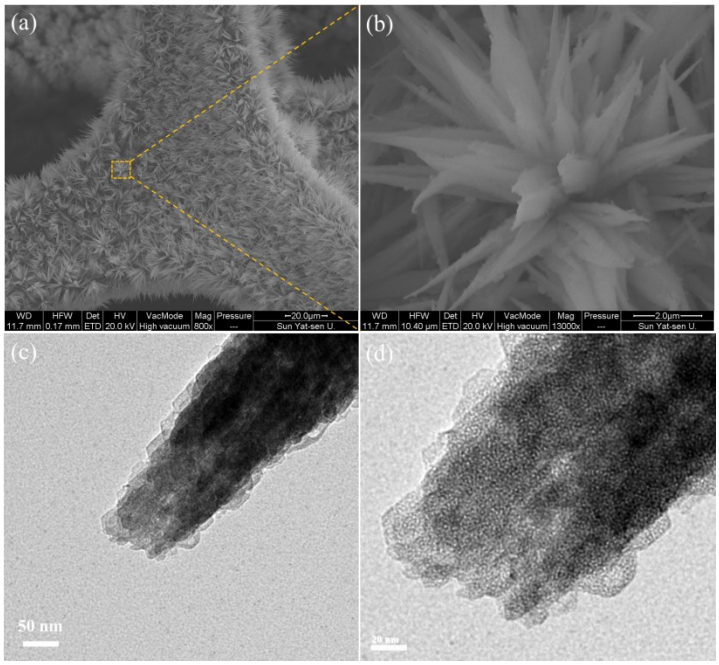

Fig. S4 (a,b) SEM images and (c,d) TEM images of Co-H NAs/NF.

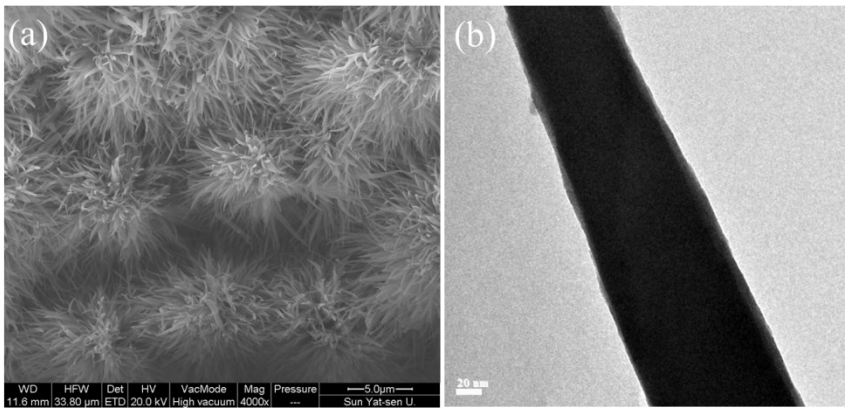

Fig. S5 SEM and TEM images of BTC-CoZnFeNi/NF.

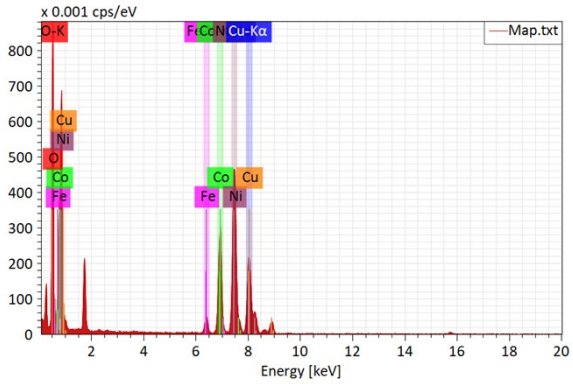

Fig. S6 EDXS spectrum of $Ni_{0.8}Fe_{0.2}$/Co-H NAs/NF separated from Ni foam.

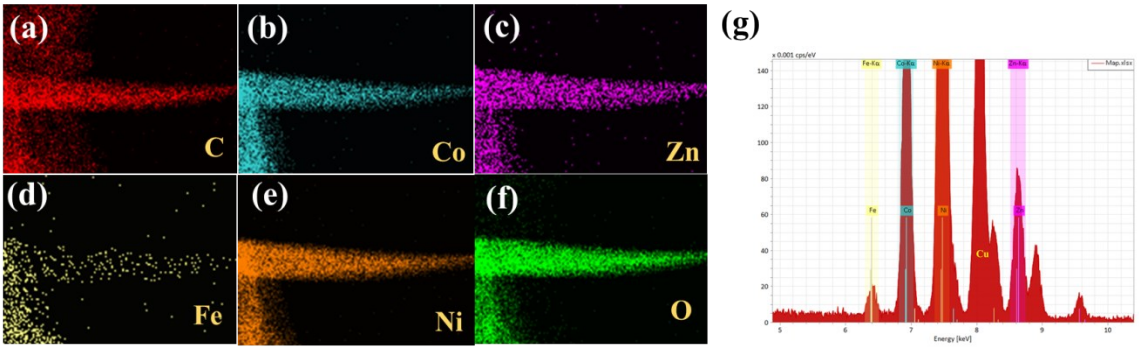

Fig. S7 EDX element mapping images and energy spectrum of BTC-CoNiFeZn/NF.

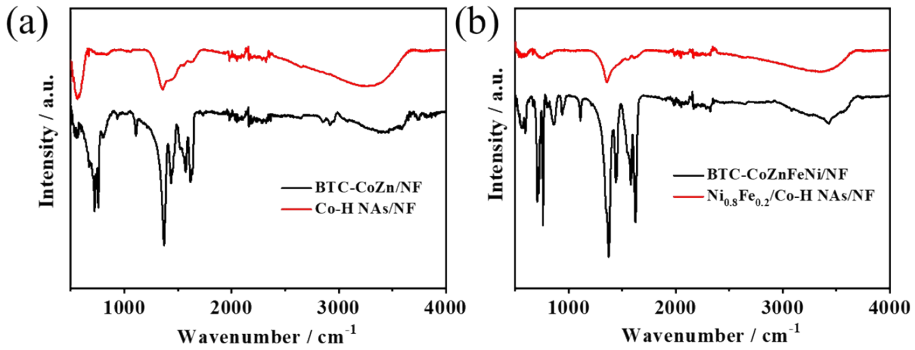

Fig. S8 FTIR of (a) BTC-CoZn and Co-H NAs/NF, (b) BTC-CoNiFeZn and $Ni_{0.8}Fe_{0.2}$/Co-H NAs/NF.

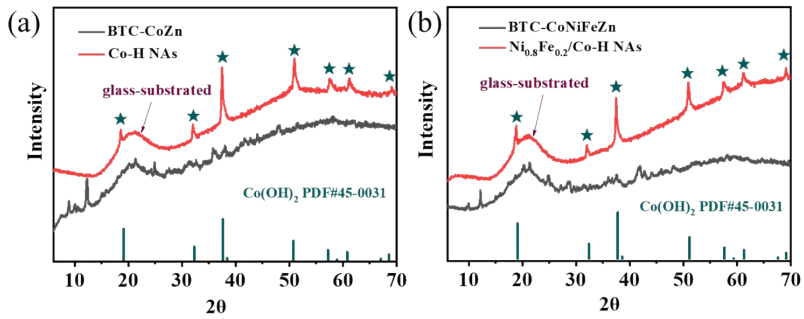

Fig. S9 XRD patterns of (a) BTC-CoZn, Co-H NAs, and (b) BTC-CoNiFeZn, $Ni_{0.8}Fe_{0.2}$/Co-H NAs that were collected from the surface of NF by ultrasound.

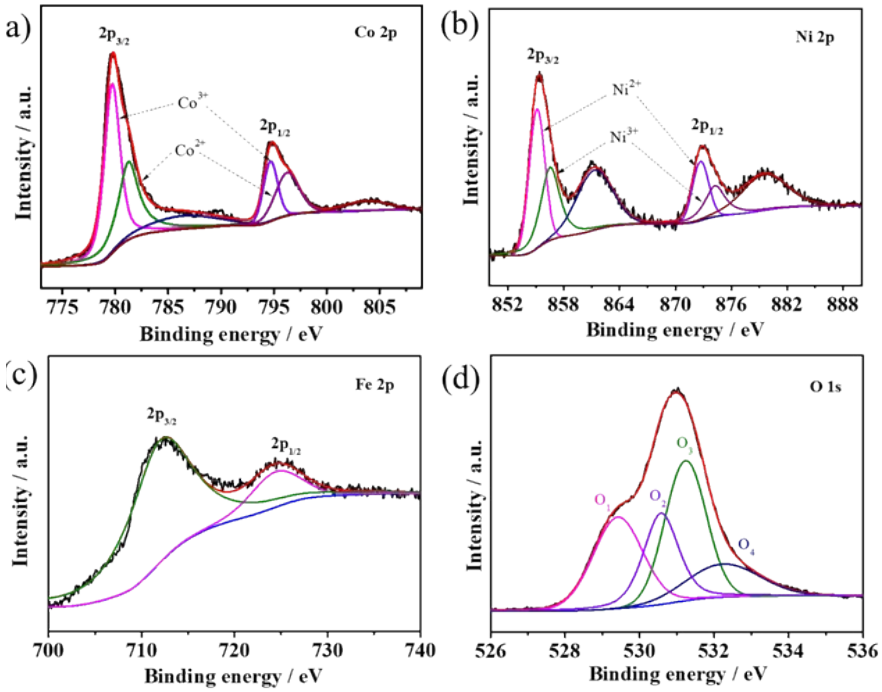

Fig. S10 High-resolution XPS spectra of Ni 2p, Co 2p, Fe 2p and O 1s of $Ni_{0.8}Fe_{0.2}$/Co-H NAs/NF.

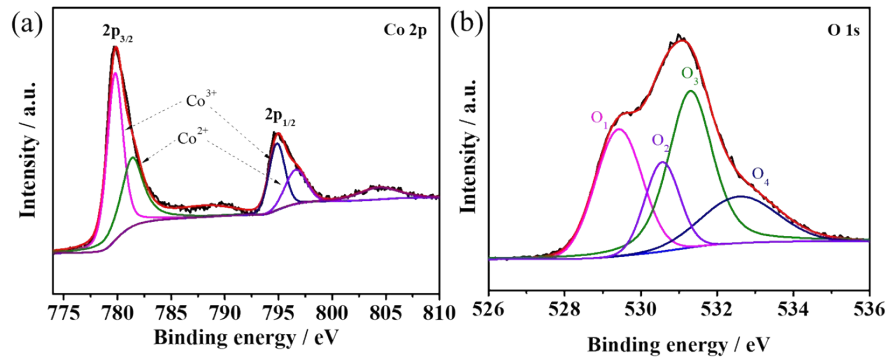

Fig. S11 High-resolution (a) Co 2p and (b) O1s XPS spectra of Co-H NAs/NF.

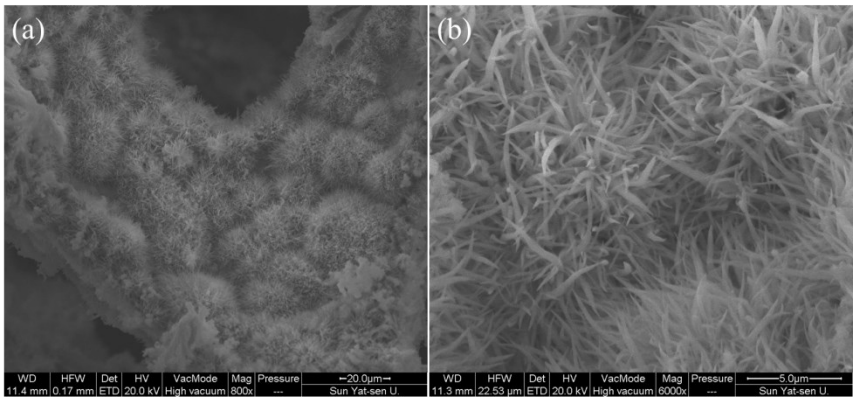

Fig.S12 SEM images of $Ni_{0.8}Fe_{0.2}$/Co-H NAs/NF after 135 h OER test in 1.0 M KOH solution.

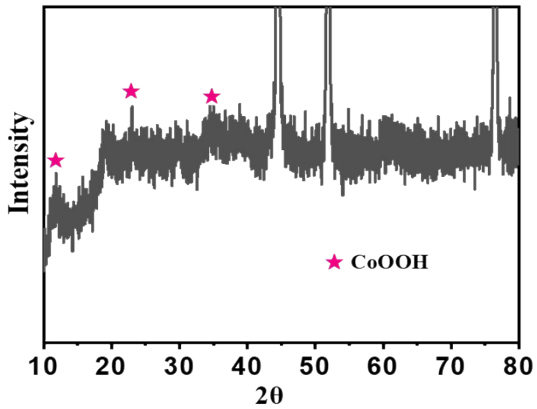

Fig. S13 XRD pattern of $Ni_{0.8}Fe_{0.2}$/Co-H NAs/NF after 135 h OER test in 1.0 M KOH solution.

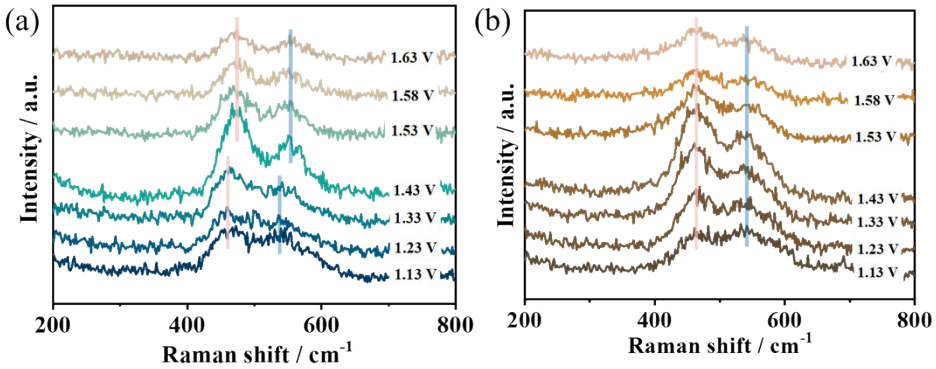

Fig. S14 In-situ Raman spectra of (a) Co-H NAs/NF and (b) $Ni_{0.8}Fe_{0.2}$/Co-H NAs/NF. The data were obtained in 0.1 M KOH used custom made teflon electrolyzer at applied potential from 1.13 to 1.63 V.

The relative strength (I_{465}/I_{537}) increases with the increasing of OER voltage, indicating the formation of oxy-hydroxide during OER tests, which is considered to be the formation of active site of Co, Ni-based catalysts.[S1,S2]

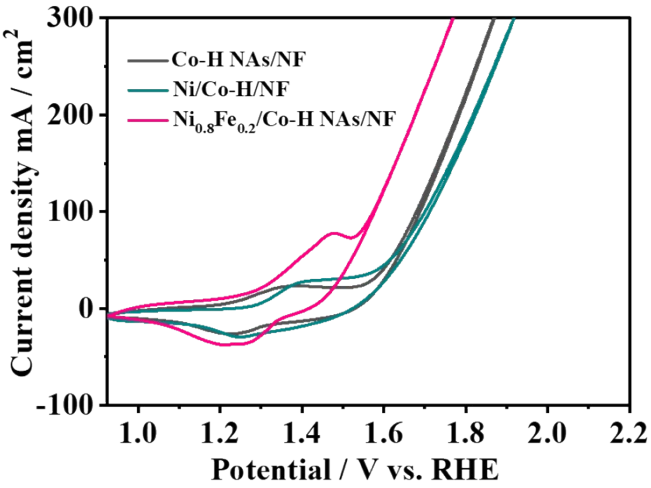

Fig. S15 CV curves of Co-H NAs/NF, Ni/Co-H/NF and $Ni_{0.8}Fe_{0.2}$/Co-H NAs/NF in 1M KOH at 10 mV/s. Ni/Co-H/NF: the preparation method is the same as Co-H NAs/NF except that $Ni(NO_3)_2$+ $Co(NO_3)_2$ (1:1) replaces $Co(NO_3)_2$.

The CV curves show that the redox peak of M (Co, Ni) shifts anodically after Fe dopants, and this phenomenon indicates a strong electronic interaction between M and Fe, which will further promote OER performance.[S3,S4]

Table S1. The summary of transition based electrocatalysts for OER.

MOFs types	Substrate	Electrolyte	η /x mA cm-2 /mV	Tafel slope / mV deg^{-1}	Refs
Co-H NAs	NF	1.0 M KOH	$293_{/20}$	58.1	This work
$Ni_{0.8}Fe_{0.2}$/Co-H NAs	NF	1.0 M KOH	$247_{/20}$ $231_{/10}$	34.2	This work
FeCo-oxyhydroxides	NF	1.0 M KOH	$331_{/10}$	42	[S5]
Co-Fe PBAs-250	GCE	1.0 M KOH	$237_{/10}$	59.7	[S6]
CoFe-MOF-OH	GCE	1.0 M KOH	$265_{/10}$	44	[S7]
NiCo-UMOFNs	GCE	1.0 M KOH	$250_{/10}$	42	[S8]
Cr-CoFe LDHs	NF	1.0 M KOH	$238_{/10}$	107	[S9]
$Ni_{0.75}Fe_{0.25}(OH)_x$	GCE	1.0 M KOH	$310_{/10}$	68	[S10]
$(Ni_2Co_1)_{0.925}Fe_{0.075}$-MOF	NF	1.0 M KOH	$257_{/10}$	41.3	[S11]
MIL-53(FeNi)	NF	1.0 M KOH	$233_{/10}$	31.4	[S12]
$CoFe(OH)_x$	GCE	1.0 M KOH	$293_{/10}$	67.4	[S13]
Fe/Ni-BTC	NF	0.1 M KOH	$270_{/10}$	47	[S14]
aMOF-NC	GCE	1.0 M KOH	$249_{/10}$	39.5	[S15]
LS-6%-NiFe-MOFs	GCE	1.0 M KOH	$230_{/10}$	86.6	[S16]
$Co_{0.5}Fe_{0.5}OOH$	NF	1.0 M KOH	$220_{/10}$	38.2	[S17]
2D NiFe-MOF	NF	0.1 M KOH	$240_{/10}$	34	[S18]
Co-MOF	NF	1.0 M KOH	$311_{/10}$	77	[S19]
$Fe_{0.33}Co_{0.67}OOH$	CFC	1.0 M KOH	$266_{/10}$	30	[S20]
Ni_5Fe LDH	NF	1.0 M KOH	$220_{/10}$	59	[S21]

GCE: Glassy carbon electrode; NF: Nickel foam; CFC: Carbon fiber cloth.

References

[S1] Z. C. Kuang, S. Liu, X. N Li, M. Wang, X. Y. Ren, J. Ding, R. L. Ge, W. H. Zhou, A. I. Rykov, M. T. Sougrati, P. E. Lippens, Y. Q. Huang, J. H. Wang, J. Energy Chem., 2021, 57, 212.

[S2] S. Lee, K. Banjac, M. Lingenfelder, X. L. Hu, Angew. Chem., 2019, 131, 10401.
[S3] L. Trotochaud, S. L. Young, J. K. Ranney, S. W. Boettcher, J. Am. Chem. Soc., 2014, 136, 6744.
[S4] M.a S. Burke, M. G. Kast, L. Trotochaud, A. M. Smith, J. Am. Chem. Soc., 2015, 137, 3638.
[S5] J. Y. Tian, F. L. Jiang, D. Q. Yuan, L. J. Zhang, Q. H. Chen, M. C. Hong, *Angew. Chem. Int. Ed.,* 2020, **59**, 2.
[S6] Q. Hu, X. W. Huang, Z. Y. Wang, G. M. Li, Z. Han, H. P. Yang, P. Liao, X. Z. Ren, Q. L. Zhang, J. H. Liu, C. X. He, *Small,* 2020, 2002210.
[S7] Z, H. Zou, T. T. Wang, X. H. Zhao, W. J. Jiang, H. R. Pan, D. Q. Gao, C. L. Xu, *ACS Catal.,* 2019, **9**, 7356.
[S8] S. L. Zhao, Y. Wang, J. C. Dong, C. T. He, H. J. Yin, P. F. An, K. Zhao, X. F. Zhang, C. Gao, L. J. Zhang, J. W. Lv, J. X. Wang, J. Q. Zhang, A. M. Khattak, N. A. Khan, Z. X. Wei, J. Zhang, S. Q. Liu, H. J. Zhao, Z. Y. Tang, Nat. Energy, 2016, 1, 16184.
[S9] L. L. Wen, X. L. Zhang, J. Y. Liu, X. Y. Li, C. C. Xing, X. J. Lyu, W. P. Cai, W. C. Wang, Y. Li, *Small,* 2019, **15**, 1902373.
[S10] T. Tian, M. Zheng, J. Q. Lin, X. Y. Meng, Y. Ding, *Chem. Commun.,* 2019, **55**, 1044.
[S11] Q. Z. Qian, Y. P. Li, Y. Liu, L. Yu, G. Q. Zhang, *Adv. Mater.,* 2019, 1901139.
[S12] F. Z. Sun, G. Wang, Y. Q. Ding, C. Wang, B. B. Yuan, Y. Q. Lin, Adv. Energy Mater., 2018, 8, 1800584.
[S13] X. Y. Yue, W. T. Ke, M. H. Xie, X. P. Shen, Z. Y. Yan, Z. Y. Ji, G. X. Zhu, K. Q. Xu, H. Zhou, Catal. Sci. Technol., 2020, 10, 215.
[S14] L. Wang, Y.Z. Wu, R. Cao, L.T. Ren, M. X. Chen, X. Feng, J. W. Zhou, B. Wang, ACS Appl. Mater. Interfaces, 2016, 8, 16736.
[S15] C. Liu, J. Wang, J. J. Wan, Y. Cheng, R. Huang, C. Q. Zhang, W. L. Hu, G. F. Wei, C. Z. Yu, Angew. Chem. Int. Ed. 2020, 59, 3630.
[S16] Q. Q. Ji, Y. Kong, C. Wang, H. Tan, H. L. Duan, W. Hu, G. N. Li, Y. Lu, N. Li, Y. Wang, J. Tian, Z. M. Qi, Z. H. Sun, F. C. Hu, W. S. Yan, ACS Catal. 2020, 10, 5691.
[S17] J. Du, C. Li, X. L. Wang, X. Y. Shi, H. P. Liang, *ACS Appl. Mater. Interfaces,* 2019, **11**, 25958.
[S18] J. J. Duan, S. Chen, C. Zhao, *Nat. Commun.*, 2017, **8**, 15341.
[S19] X. Q. Zhang, W. D. Sun, H. T. Du, R. M. Kong, F. L. Qu, *Inorg. Chem. Front.*, 2018, **5**, 344.
[S20] S. H. Ye, Z. X. Shi, J. X. Feng, Y. X. Tong, G. R. Li, *Angew. Chem. Int. Ed.,* 2018, **57**, 2672.
[S21] Y. Zhang, Q. Shao, Y. Pi, J. Guo, X. Q. Huang, *small,* 2017, **13**, 1700355.